

Discrete Spectra and Continuous Spectrum of the Barotropic Quasi-Geostrophic Model—A Calculation of Meteorological Data^①

Zhang Minghua (张明华)

Institute for Terrestrial and Planetary Atmospheres, State University of New York at Stony Brook

Zeng Qingcun (曾庆存)

Institute of Atmospheric Physics, Chinese Academy of Sciences, Beijing 100080

(Received May 6, 1999)

ABSTRACT

Atmospheric disturbances at 300 hPa are decomposed into normal modes, referred as discrete-spectrum disturbances which can propagate freely in the observed zonal mean flow, and non-modal transient disturbances, referred as continuous-spectrum disturbances which are continuously sheared and eventually absorbed by the zonal flow. It is shown that normal modes represent only a small fraction of the observed atmospheric disturbances, while continuous-spectrum disturbances represent the majority of observed disturbances, even when the basic flow is unstable.

Daily variabilities of the observed continuous-spectrum disturbances are presented. They are shown to follow the results of wave-packet theory. Calculations suggest that there are abundant sources to excite continuous-spectrum disturbances in the atmosphere.

Key words: Normal mode, Discrete-spectrum, Continuous-spectrum, Wave-packet

1. Introduction

Maintenance, development and decay of middle latitude atmospheric disturbances are central to the understanding of synoptic weather processes and short-term climate variability. Frontogenesis and surge of cold waves are typically associated with rapid development of favorably configured small disturbances in the upper troposphere. These disturbances further act as interactive transient forcing to cause low frequency variabilities. They also affect the intensity of westerlies and the equator-to-pole temperature gradient of the atmosphere.

Studies of small disturbances have traditionally used the normal mode method (e.g. Eady, 1949; Charney, 1947), in which disturbances are treated as a sum of various characteristic waves, or normal modes. These waves can either propagate freely in the background flow, or decay and develop exponentially. However, recent studies of atmospheric disturbances have called meteorologists' attention to the non-modal form of atmospheric motions (e.g. Zeng, 1979; Farrell, 1982, 1984, 1985; Held, 1985). The non-modal disturbances represent transient and dispersive eddy motions that are continuously sheared by the basic flow. It

^①This research was partly supported by the Institute of Atmospheric Physics, Chinese Academy of Sciences. Additional support is provided by NASA Grant NAGW3517 and DOE Grant DEFG0285-ER60314 to SUNY at Stony Brook.

has been shown that this form of disturbances can account for rapid disturbance growth within a stable basic flow, and they resemble more to the actual structures of observed atmospheric disturbances.

Given the apparent success of the normal mode approach in explaining certain aspects of atmospheric phenomena, and evidences that non-modal forms of disturbances are probably more representative of the real atmosphere, a question naturally arises: How much of the observed atmospheric disturbance belongs to modal forms of motion and how much of it belongs to non-modal forms of motion? The present study uses the approach in Zhang and Zeng (1997, referred as ZZ1) to project observed atmospheric disturbances onto modal and non-modal components. The purpose is to quantitatively clarify the magnitudes of modal and non-modal components of disturbances in the real atmosphere, which has been previously studied only in idealized models (e.g. Farrell, 1982, 1988; Farrel and Ioannou, 1993).

In ZZ1, it was shown that the free evolution of an initial disturbance in a shear basic flow can be described by the sum of discrete spectrum disturbances (modal form) and continuous spectrum disturbances (non-modal form), with each of them expressed as spectral functions of the discrete spectra and continuous spectrum functions of an atmospheric model. Since the real atmosphere is subject to various external and internal forcings, the behavior of the observed disturbances must differ from either the discrete or continuous spectrum disturbances that are described by a free model. Yet, if the forcings are sufficiently small or the time period examined is short, partition of observed disturbances into modal and non-modal parts can provide an approximate prediction of the evolutionary processes of disturbances. This information has practical importance in initializations of numerical weather prediction. The partition also provides insights about the nature of atmospheric forcings.

The paper is organized in the following order. The second section gives a brief description of the theoretical framework to decompose atmospheric disturbances into modal and non-modal components. The following section presents the decomposition results, including time evolution of the decomposed components, and the partition of energy and generalized enstrophy. The last section summarizes the results. An appendix is included to show an alternate approach of energy decomposition by using spectral functions of the adjoint model.

2. Decomposition of atmospheric disturbances into discrete- and continuous-spectrum disturbances

We first outline the dynamic framework from which the decomposition of atmospheric disturbances is made. A detailed discussion of the theory can be found in ZZ1. If an initial vorticity field $\zeta'|_{t=0} = \zeta'_0$ is released into a basic flow \bar{v}_λ , and it follows the barotropic quasi-geostrophic model on a sphere:

$$\left(\frac{\partial}{\partial t} + \frac{\bar{v}_\lambda}{a \sin \theta} \frac{\partial}{\partial \lambda}\right) \zeta' + v'_\theta \frac{\partial \bar{\zeta}}{a \partial \theta} = 0, \quad (1)$$

where

$$\zeta' = \frac{1}{a^2 \sin \theta} \frac{\partial}{\partial \theta} \sin \theta \frac{\partial \psi'}{\partial \theta} + \frac{1}{a^2 \sin^2 \theta} \frac{\partial^2 \psi'}{\partial \lambda^2}, \quad v'_\theta = \frac{\partial \psi'}{a \sin \theta \partial \lambda}, \quad (2)$$

its evolution can be expressed as (see ZZ1)

$$\psi'(\lambda, \theta, t) = \psi'_d(\lambda, \theta, t) + \psi'_c(\lambda, \theta, t)$$

$$= \sum_k \sum_l A_l^k G_l^k(\theta) e^{ik(\lambda - c_l^k t)} + \sum_k \int_{\lambda_{\min}}^{\lambda_{\max}} B^k(c) G^k(\theta, c) e^{ik(\lambda - ct)} dc, \quad (3)$$

$G_l^k(\theta)$ satisfies the following equation and boundary conditions:

$$(\bar{\lambda}(\theta) - c_l^k) \left(\frac{1}{\sin\theta} \frac{d}{d\theta} \sin\theta \frac{dG_l^k}{d\theta} - \frac{k^2}{\sin^2\theta} G_l^k \right) - \frac{1}{\sin\theta} \frac{d\bar{\lambda}}{d\theta} G_l^k = 0 \quad (4)$$

$$G_l^k \Big|_{\theta=0, \pi} = 0, \quad (5)$$

where $\bar{\lambda}(\theta) = \bar{v}_\lambda / (a \sin\theta)$, and the eigenvalue c_l^k is outside the interval of $[\bar{\lambda}_{\min}, \bar{\lambda}_{\max}]$. $G_l^k(\theta)$ is defined as spectral functions of the discrete spectra of the model since c_l^k s are isolately distributed. In ZZ1, it has been shown that the number of c_l^k for a given k is limited beyond any sufficiently small neighbor of $[\bar{\lambda}_{\min}, \bar{\lambda}_{\max}]$. $G_l^k(\theta)$ is the same as the commonly referred normal modes. The disturbance $\psi'_d(\lambda, \theta, t)$ that is entirely described by normal modes or a modal solution is called the discrete-spectrum disturbance.

$G^k(\theta, c)$ also satisfies (4)–(5), but the associated c covers the whole interval of $[\bar{\lambda}_{\min}, \bar{\lambda}_{\max}]$. It is called a spectral function of the continuous spectrum, and it has first-order discontinuities. The disturbance $\psi'_c(\lambda, \theta, t)$ that is entirely described by spectral functions of the continuous spectrum represents the non-modal form of the solution. It is called a continuous spectrum disturbance. Following the Riemann–Lebesgue lemma, as $t \rightarrow \infty$, $\psi'_c(\lambda, \theta, t) \rightarrow 0$, even though the disturbance can have substantial growth at an initial stage (e.g. Farrell, 1984, 1985; Lu et al., 1986).

The solution given in (3) not only describes the evolutionary process of small disturbances — complete with both modal and non-modal motions, but also provides a basis for decomposition of a disturbance field. If t is set to zero, (3) gives a complete expansion of any given disturbance in terms of spectral functions of the discrete and continuous spectrum of the model. Numerically, if the grids from co-latitude $\theta=0$ to $\theta=\pi$ are represented by $\theta_1, \theta_2, \dots, \theta_{J+2}$ (inclusive of the boundary grids), a complete set of eigenfunctions (vectors) can be obtained from (4)–(5) for a given zonal wave number $k \neq 0$ as $\{G_l^k, l=1, 2, \dots, J\}$ where

$$G_l^k = [G_l^k(\theta_2), G_l^k(\theta_3), \dots, G_l^k(\theta_{J+1})]^T. \quad (6)$$

It can be shown that the numerically calculated G_l^k s are weighted-orthogonal to each other in the analog to (39) in ZZ1 (also see Held, 1985; Lu et al., 1986):

$$(G_l^k, G_{l'}^k)_n = \sum_{j=2}^{J+1} Q_l^k(\theta_j) Q_{l'}^k(\theta_j) \frac{1}{\bar{\beta}_j} t \cdot y = 0, \quad (7)$$

when $l \neq l'$, where $y = \cos\theta$, and $\bar{\beta}_j = (d\bar{\lambda}/d\theta)_j$, $Q_l^k = DG_l^k$ which represents the finite difference form of the vorticity of eigenfunction G_l^k ; D is the finite difference analog to (46) in ZZ1. This set of basis functions can be normalized by letting

$$(G_l^k, G_l^k)_n = 1. \quad (8)$$

For an observed disturbance vorticity field and stream function

$$\zeta'(\lambda, \theta) = \sum_k \zeta^k(\theta) e^{ik\lambda}, \quad \psi'(\lambda, \theta) = \sum_k \psi^k(\theta) e^{ik\lambda}, \quad (9)$$

where $k = \pm 1, \pm 2, \dots$, and ζ^k satisfies the following boundary conditions

$$\zeta^k(\theta = 0) = \zeta^k(\theta = \pi) = 0. \quad (10)$$

Hence, if

$$\psi^k = (\psi^k(\theta_2), \psi^k(\theta_3), \dots, \psi^k(\theta_{J+1}))^T = \sum_i A_i^k \mathbf{G}_i^k = \psi_d^k + \psi_c^k, \quad (11)$$

then

$$\zeta^k = (\zeta^k(\theta_2), \zeta^k(\theta_3), \dots, \zeta^k(\theta_{J+1}))^T = \sum_i A_i^k \mathbf{Q}_i^k = \zeta_d^k + \zeta_c^k. \quad (12)$$

Thus, the coefficients A_i^k can be calculated by

$$A_i^k = (\zeta^k, \mathbf{Q}_i^k)_n = \sum_j \zeta^k(\theta_j) \mathbf{Q}_i^k(\theta_j) \frac{\sin \theta_j}{\beta_j} \Delta y. \quad (13)$$

ψ_d^k and ψ_c^k are the projections of the disturbance ψ^k on the discrete-spectrum functions and the computationally distorted continuous-spectrum functions.

3. Results of decomposition

3.1 Mean states

We first present results of decomposing the time-averaged 300 hPa stream functions. The decomposed states carry the information of stationary forcing of the discrete- and continuous-spectrum disturbances. In addition, the decomposition serves to illustrate the patterns of, and the difference between the two types of disturbances. Fig. 1(a) shows the mean disturbance stream function of January 1982 on 300 hPa. The zonal flow used is January averaged one (the same as in Fig. 4a of ZZ1). As expected, stronger eddy activities are found in the Northern Hemisphere than those found in the Southern Hemisphere for this season. Cyclonic eddy motions (positive disturbance vorticity) prevail at the locations of the troughs of the three planetary stationary waves in the Northern Hemisphere, namely, near the east coasts of Asia and North America, and to the east of Europe (Wallace et al., 1983).

Figures 1b and 1c show the corresponding discrete- and continuous-spectrum disturbances. It is seen that the discrete-spectrum component of the disturbances has very large spatial scales, with wavenumber one dominant in the zonal direction, and wavenumber two in the meridional direction. On the contrary, the continuous-spectrum component captures virtually all synoptic-scale structures in the total disturbance field. Difference between Figs. 1a and 1b is appreciable only in the subtropics. This suggests that there are rich sources of forcing to excite non-modal forms of disturbances in the atmosphere. These could be forcings from surface boundaries, featuring localized characteristics, or from atmospheric internal heating, or from non-linear wave-wave and wave-mean flow interactions. On the other hand, the modal forms of motion in the atmosphere are probably excited by continental scale land-ocean contrast.

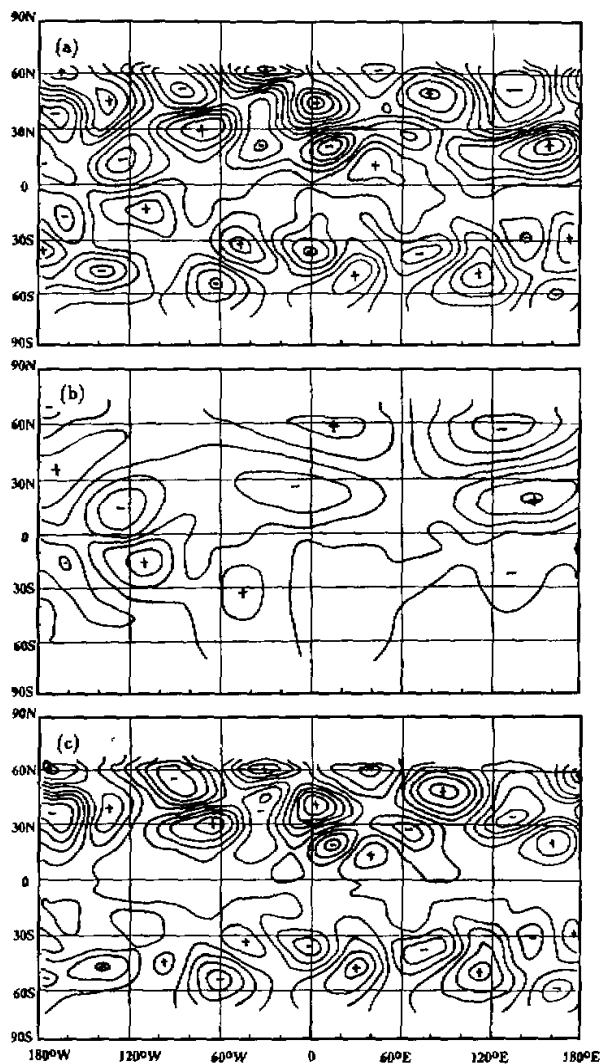


Fig. 1. Disturbance stream function of the monthly averaged flow for January 1982 at 300 hPa (contour interval: $5 \times 10^6 \text{ m}^2/\text{s}$). (a) total disturbances, (b) discrete-spectrum disturbances, (c) continuous-spectrum disturbances.

Since the decompositions are made based on linear theory with zonal mean basic flow, it is possible to examine the discrete- and continuous-spectrum disturbances by using different zonal wavenumbers. Figure 2a shows the latitudinal distribution of the amplitude and phase of the discrete-spectrum disturbance for zonal wavenumbers 1 to 5. Consistent with Fig. 1b, large amplitudes in middle to high latitudes are restricted to wavenumbers 1 and 2. For wavenumber larger than 3, the disturbances are confined in low latitudes. Note that these low-latitude confined disturbances have simple phase structures and are asymmetric to the

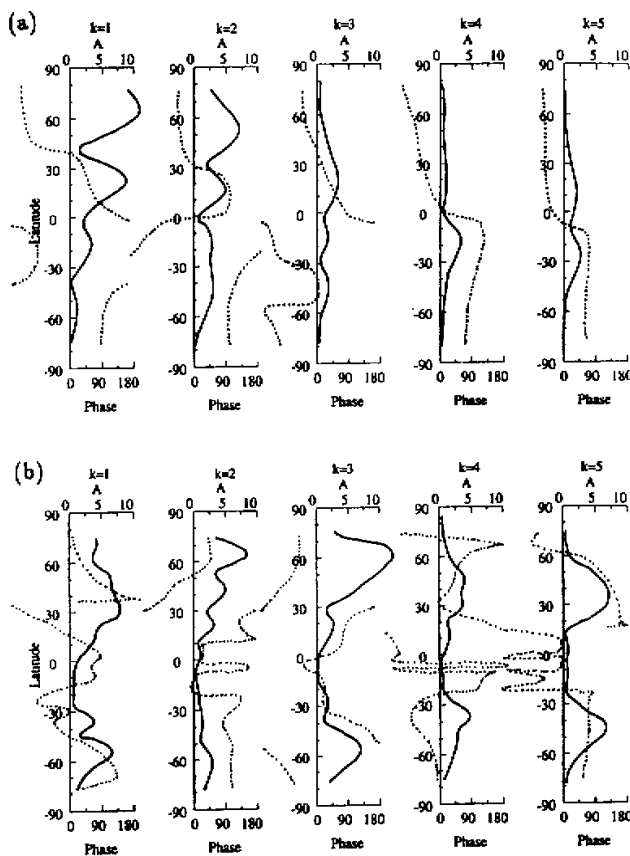


Fig. 2. Meridional distribution of the amplitude (solid, unit: $10^6 \text{ m}^2/\text{s}$) and phase (dotted) of stream functions for zonal wavenumbers $k=1$ to $k=5$ in January 1982. (a) discrete-spectrum disturbances, (b) continuous-spectrum disturbances.

equator. Figure 2b gives the amplitude and phase of continuous-spectrum disturbances for various zonal wavenumbers. For zonal wavenumbers $k=1$ and $k=2$, the magnitude of continuous-spectrum disturbances is comparable with that of the discrete-spectrum disturbances. But for larger zonal wavenumbers, the amplitude of the continuous-spectrum component is much larger in middle and high latitudes; and they exhibit complicated meridional structures.

Figure 3a is the observed mean disturbance stream function in July 1982 at 300 hPa. The corresponding decompositions of ψ' into ψ'_c and ψ'_d are given in Figs. 3b and 3c. The discrete-spectrum component has a basic wavenumber one structure in both the zonal and meridional directions. The continuous-spectrum component, once again, resembles closely to the total disturbances in many details; in particular, it captures the majority of disturbances embedded in the middle latitude jet cores.

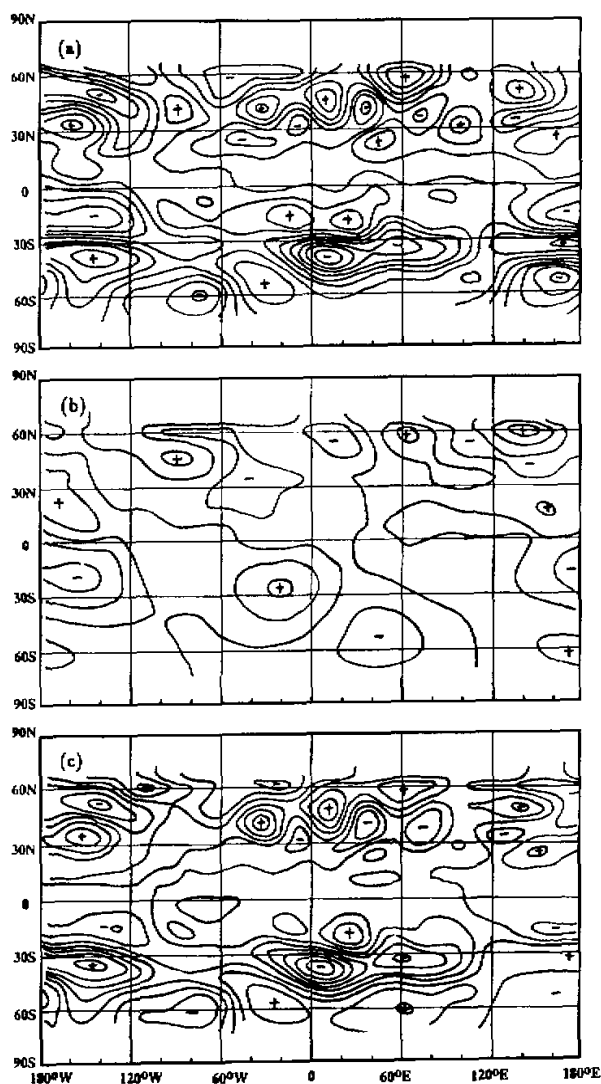


Fig. 3. Same as Fig. 1 except for July 1982.

Meridional profiles of $|\psi'_d|$ and $|\psi'_e|$ for different zonal wavenumbers in July 1982 are shown in Figs. 4a and 4b respectively. Also shown are the phase structures of the separated components. The relative contributions of the continuous-spectrum disturbance are much larger than that of discrete-spectrum disturbance when the zonal wavenumber is larger than 3.

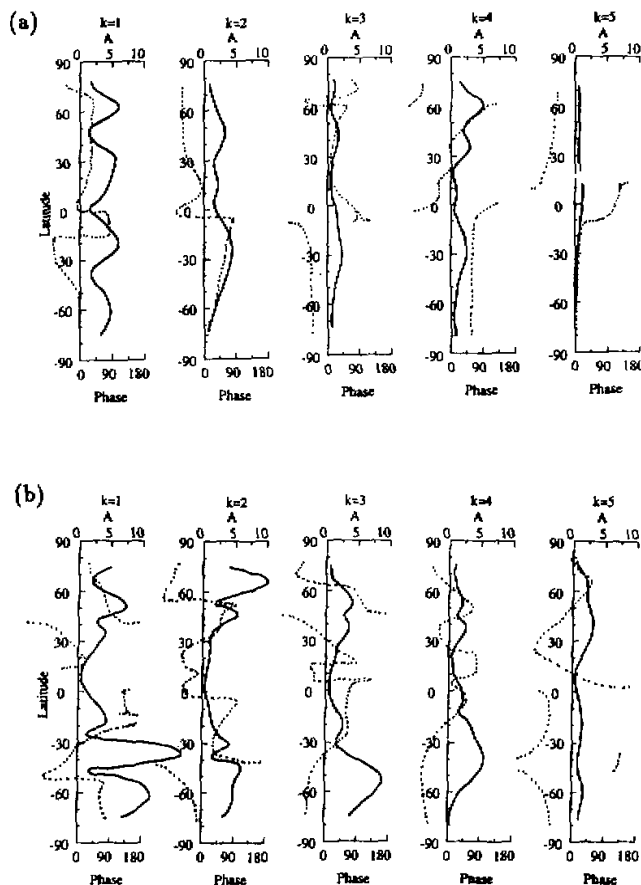


Fig. 4. Same as Fig. 2 except for July 1982.

3.2 Evolution of disturbances

If we consider the observed disturbance stream function on a given day as an initial condition $\psi'_0(\lambda, \theta)$, with an initial vorticity field ζ'_0 , and if the evolution of the disturbance ψ' can be described by (1), then the time variation of ψ' follows $\psi'(\lambda, \theta, t) = \psi'_d(\lambda, \theta, t) + \psi'_c(\lambda, \theta, t)$. The characteristics of the discrete-spectrum disturbance ψ'_d , describing the neutral or unstable normal modes, have been discussed in many previous theoretical studies. In real observations, freely travelling waves in the atmosphere have been reported by Madden (1979), Kasahara (1976) and Ahlquist (1982). However, their magnitudes are very small in comparison with observed atmospheric variances (Wallace and Blackman, 1983). Using the decomposed discrete-spectrum component of observed disturbances, it is possible to give a quantitative measure of all the normal modes combined. Figure 5 shows a time series of the observed discrete-spectrum disturbances on 300 hPa superimposed on the mean zonal flow for three days in January 1982 (days 1, 2, and 4). It is seen that the magnitudes of free wave

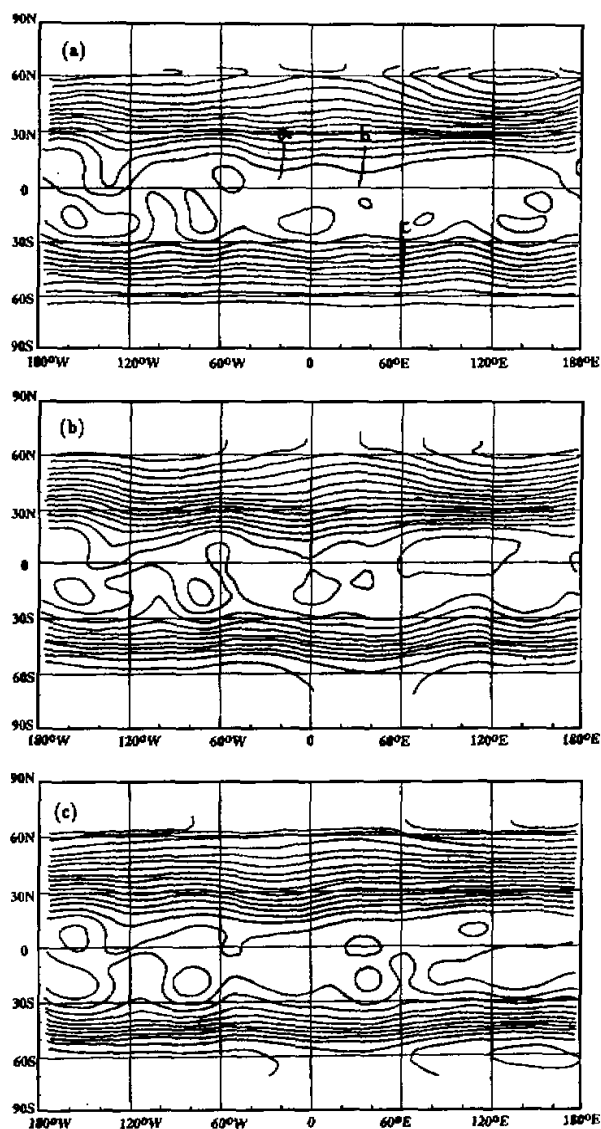


Fig. 5. Time variation of observed 300 hPa discrete-spectrum disturbances superimposed on the mean zonal flow (contour intervals: $10 \times 10^6 \text{ m}^2/\text{s}$) in January 1982. (a) January 1, (b) January 2, and (c) January 4.

activities are very weak. There are indications of wave propagations. For example, two synoptic-scale troughs in the Northern Hemisphere (labelled as a and b) moved eastward from day 1 to day 2; the trough of a weak middle planetary wave in the Southern Hemisphere (labelled c) moved westward from about 60°E in day 1 to 30°E in day 4. However, since the discrete-spectrum disturbances shown here include modes with all zonal scales and

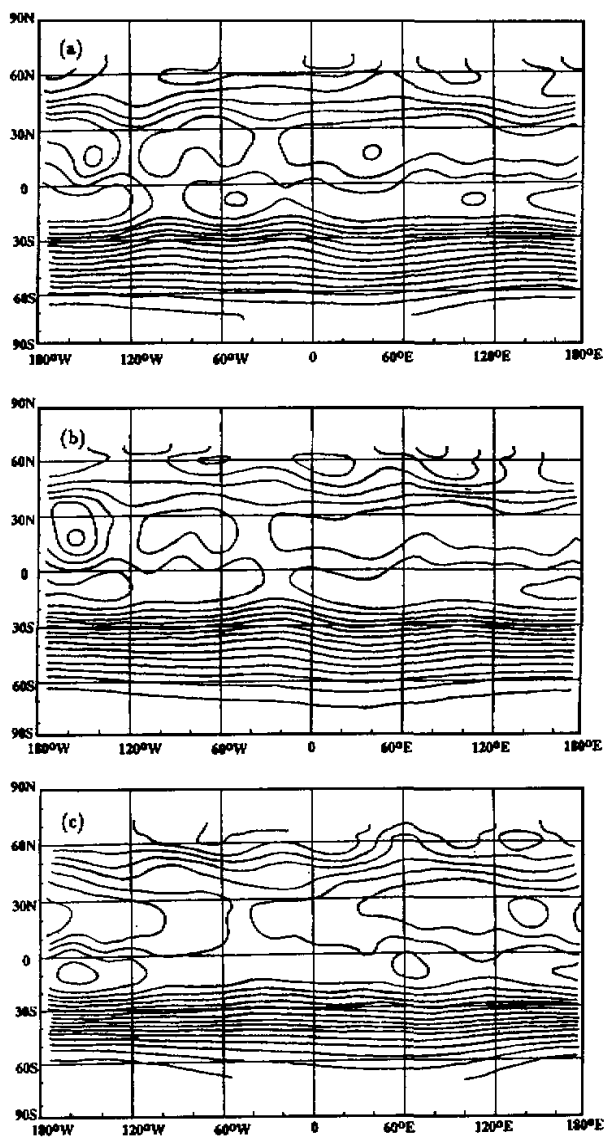


Fig. 6. Same as Fig. 5 except for July 1982.

meridional scales, and furthermore, there must be influences of external forcing on the modes, it is not fruitful to attempt to identify the individual modes from this figure. These figures show the combined magnitude of all the daily free travelling waves in the atmosphere, which will be contrasted with the magnitude of continuous-spectrum disturbances on the same days. Figure 6 shows the corresponding figure in July 1982. Free wave activities are even weaker. It should be pointed out that in July 1982, the 300 hPa zonal flow is barotropically

unstable as discussed in ZZ1.

The original form of the continuous-spectrum component

$$\psi'_c(\lambda, \theta, t) = \sum_k \int_{\lambda_{\min}}^{\lambda_{\max}} B^k(c) G^k(\theta, c) e^{ik(\lambda - ct)} dc$$

can be represented by a combination of wave packets (Zeng et al., 1986):

$$\begin{aligned} \psi'_c(\lambda, \theta, t) &= \sum_k \sum_l \int_{c_l - \delta c/2}^{c_l + \delta c/2} B^k(c) G^k(\theta, c) e^{ik(\lambda - ct)} dc \\ &= \sum_k \sum_l B_l^k(\theta, \epsilon_l) e^{ik(\lambda - c_l^* t)} = \sum_k \sum_l \varphi_{cl}^k, \end{aligned} \quad (14)$$

where $k \pm 1, \pm 2, \dots, \lambda_{\min} + \delta c/2 \leq c_l^* \leq \lambda_{\max} - \delta c/2$, and

$$B_l^k(\theta, \epsilon_l) = \int_{c_l - \delta c/2}^{c_l + \delta c/2} B^k(c) G^k(\theta, c) e^{ik(c_l - c)t} dc \quad (15)$$

is a slowly varying function of t . ϵ_l is a small parameter proportional to δc . Each wave packet has a phase speed c_l^* and amplitude B_l^k varying slowly with time. Therefore, the evolutionary properties of continuous-spectrum disturbances can be examined using results from the wave packet theory. In the Northern Hemisphere, a wave packet located on the side of $d\lambda/d\theta > 0$ with northeast-southwest oriented trough-ridge lines, or located on the side of $d\lambda/d\theta < 0$ but with northwest-southeast oriented trough-ridge lines, is a developing one. On the contrary, a packet on the side of $d\lambda/d\theta > 0$ but with northwest-southeast oriented trough-ridge lines, or on the side of $d\lambda/d\theta < 0$ but with northeast-southwest oriented trough-ridge lines, is a decaying packet (Lu and Zeng, 1981; Zeng, 1983a, 1983b).

Figure 7 shows the time series of continuous-spectrum disturbances on 300 hPa superimposed on the basic flow on three days at the beginning of January in 1982 (days 1, 2, and 4). In the Northern Hemisphere, troughs denoted by a and b are developing from day 1 to day 2; trough c develops from day 1 to day 2 and then decays; trough d decays from day 1 to day 4. In the Southern Hemisphere, the three troughs labelled e to g all have decaying structures and they significantly weaken from day 1 to day 4. These characteristics are quantitative illustrations of the wave packet results in the interpretation of daily variability of observed disturbances.

Figure 8 shows the time series of continuous-spectrum component of disturbances in the corresponding July 1982. Major disturbances are in the Southern Hemisphere. Starting from day 1 (Fig. 8a), most of the disturbances in the Southern Hemisphere exhibit decaying structures according to the wave-packet theory, except for the small trough near east coast of Africa around 45°E . By day 2 (Fig. 8b), the small trough has grown to merge with an existing trough to the east, and all other major troughs and ridges remain similar to those in the previous day. But by day 4 (Fig. 8c), it is seen that most of the troughs and ridges have dramatically weakened. At the meantime, the westerly is strengthened. This is consistent with Zeng and Zhang (1999) who show that continuous-spectrum disturbances carry out most of the angular momentum transport and contribute the most to the maintenance of the westerly flow.

According to the Riemann-Lebesgue Lemma, and consistent with the wave packet theory, it can be inferred from (3) that the free continuous-spectrum disturbances should

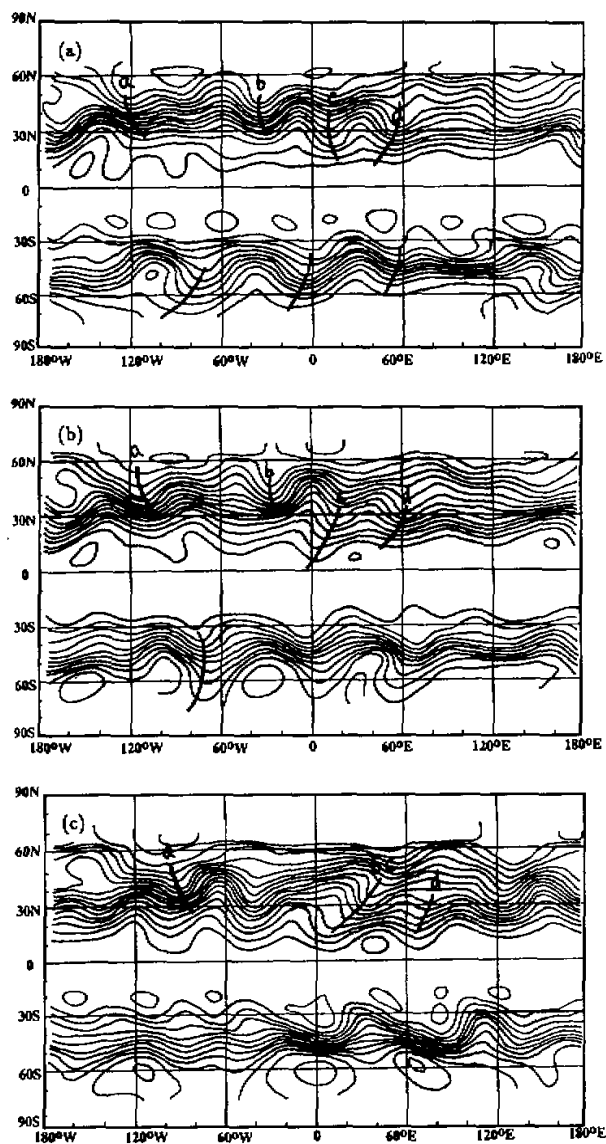


Fig. 7. Time variation of observed 300 hPa continuous-spectrum disturbances superimposed on the mean zonal flow (contour intervals: $10 \times 10^6 \text{ m}^2/\text{s}$) in January 1982. Troughs referred in the text are labelled. (a) January 1, (b) January 2, and (c) January 4.

eventually decay to approach zero magnitude (Zeng et al., 1986; Lu et al., 1986), although initial growth can take place to a significant degree (Lu et al., 1981, 1986; Zeng, 1983, a,b;

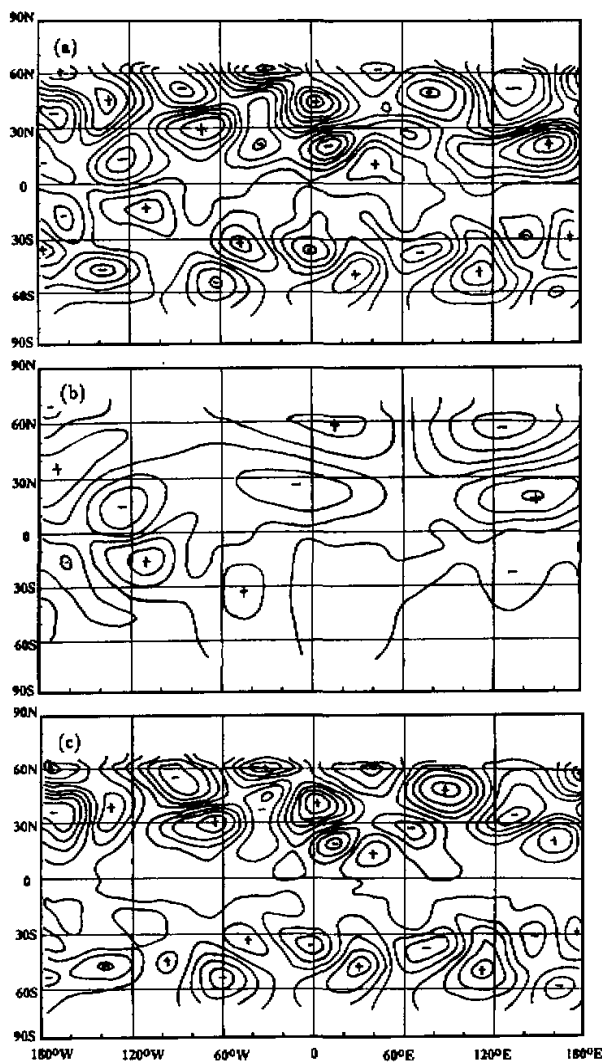


Fig. 8. Same as Fig. 7 except for July 1982.

Farrell, 1982). This feature has been also numerically confirmed by Zeng et al. (1981)^① in which a free disturbance is constructed by using the linear combination of continuous-spectrum functions and it is absorbed by the basic flow after several days of integration. Figures 5 to 8 also illustrate that continuous-spectrum disturbances dominate the total disturbance field on any given day. This, together with the final fate of free continuous-spectrum disturbances, suggests rich sources of external forcings to excite continuous-spectrum disturbances in the atmosphere.

^①Zeng, Held, and Holloway 1981, unpublished results

3.3 Partition of energy and generalized enstrophy

We now examine the partition of energy among the decomposed components. Such partition often provides a useful measure of the energy distribution, and therefore energy sources and sinks, of the different components. Since energy is a quadratic quantity, if the decomposed components are not orthogonal, then the energy cannot be partitioned exactly into the same components. This is the case for the decomposition of disturbances into discrete- and continuous-spectrum disturbances. Nevertheless, if one modifies the basis functions appropriately, namely, using the spectral functions of model (3) as one set of basis functions and those of the adjoint model of (3) as another set of basis functions, one can project the velocities in the kinetic energy quantity using two sets of basis functions, corresponding to the same discrete spectra and continuous spectrum. The disturbance kinetic energy can then be written as the sum of two terms representing the discrete- and continuous-spectrum disturbances separately. The derivation of this procedure is included in the Appendix. In the following discussion, we still use the spectral functions of (3) as the only basis functions to project the velocities. Since the energy associated with pure discrete-spectrum disturbances is small, it can be expected that the contribution of the cross product of the discrete- and continuous-spectrum disturbances to the total energy is also small.

The total energy can be written as:

$$E = \int_0^\pi \int_0^{2\pi} \frac{1}{2} [(v'_{\lambda,d} + v'_{\lambda,c})^2 + (v'_{\theta,d} + v'_{\theta,c})^2] a^2 \sin\theta d\lambda d\theta = E_d + E_r, \quad (16)$$

where E_d is the kinetic energy of the pure discrete-spectrum disturbances:

$$E_d = \int_0^\pi \int_0^{2\pi} \frac{1}{2} [(v'_{\lambda,d})^2 + (v'_{\theta,d})^2] a^2 \sin\theta d\lambda d\theta, \quad (17)$$

and $E_r = E - E_d$ is the residual:

$$E_r = \int_0^\pi \int_0^{2\pi} \left\{ \frac{1}{2} [(v'_{\lambda,c})^2 + (v'_{\theta,c})^2] + v'_{\lambda,d} v'_{\lambda,c} + v'_{\theta,d} v'_{\theta,c} \right\} a^2 \sin\theta d\lambda d\theta. \quad (18)$$

Furthermore, if the disturbance is represented in the form of Fourier series $e^{ik\lambda}$, we can write:

$$E = \sum_{k=1,2,\dots} E^k = \sum_{k=1,2,\dots} E_d^k + \sum_{k=1,2,\dots} E_r^k = E_d + E_r, \quad (19)$$

where E_d^k is the spectral power of the pure discrete-spectrum disturbances, and E_r^k is that of the residual energy for wavenumber k . Note that if E_d^k and E_d are small, E_r^k and E_r are contributed mostly by continuous-spectrum disturbances alone. There is also cancellation between $v'_{\lambda,d} v'_{\lambda,c}$ and $v'_{\theta,d} v'_{\theta,c}$ in (1) in our calculation.

Figure 9a shows E^k as a function of zonal wavenumber k in the first ten days of January 1982 (the ordinate scale is the days). In the ten-day period, maximum energy has shifted from wavenumber 5 in days 1 and 2 to wavenumber 3 in day 9, featuring the shift of synoptic wave activities to planetary wave activities. Figures 9b and 9c show the corresponding distribution of E_d^k and E_r^k . Except for wavenumbers 1 and 2 in the late part of the period, E_r^k is much

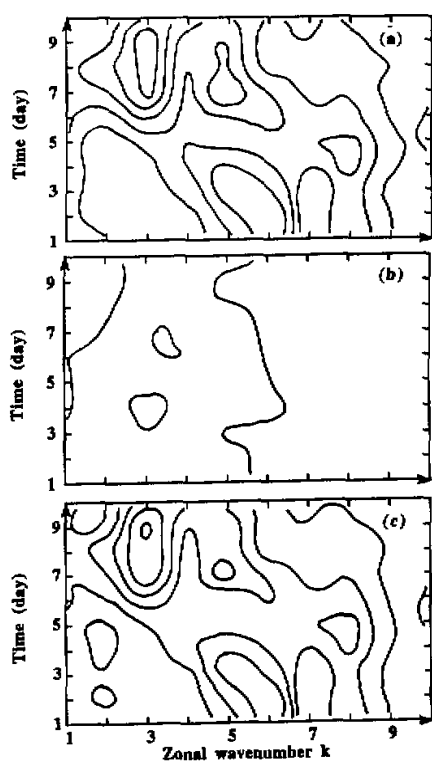


Fig. 9. Time variation of kinetic energy for different zonal wavenumbers in the first ten days of January 1982 (unit: $10^{12} \text{ m}^2/\text{s}^2$, interval is 5). (a) E^k of total disturbances, (b) E_d^k of discrete-spectrum disturbances, (c) E_r^k of residuals.

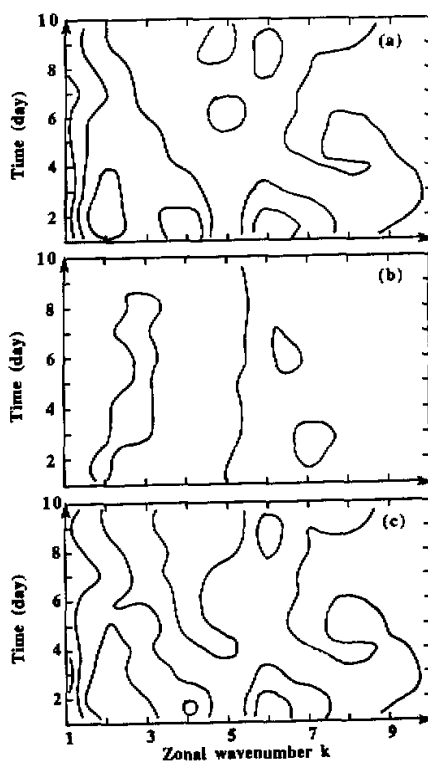


Fig. 10. Same as Figure 9 except for July 1982.

larger than E_d^k , and it accounts for the energy cascade from synoptic waves to planetary waves. This is consistent with the previous results that continuous-spectrum disturbance is dominant in the real atmosphere.

Figure 10 shows the energy distribution and the decomposed values in the first ten days of July 1982. Maximum wave energies are concentrated around zonal wavenumbers 2–4, and 6, although the basic flow is unstable to modes wave zonal wavenumbers 1, and 3 to 5. Similar to January, energy in the discrete-spectrum disturbances is negligible in comparison with that associated with the continuous-spectrum disturbances.

We next show the partition of enstrophy between the continuous- and discrete-spectrum disturbances. To make the decomposition orthogonal, we employ the weighted enstrophy (Zeng, 1982; 1983, a,b) rather than the enstrophy itself. From the basic governing equation (1), we have the conservation of the following total weighted enstrophy, $dF/dt = 0$,

where

$$F = \int_0^\pi \int_0^{2\pi} [\zeta'^2 / (-\partial \bar{\zeta} / a \sin \theta \partial \theta)] a^2 \sin \theta d\theta d\lambda. \quad (20)$$

It follows from the weighted orthogonality that

$$\begin{aligned} F = F_d + F_c = & \int_0^\pi \int_0^{2\pi} [\zeta_d'^2 / (-\partial \bar{\zeta} / a \sin \theta \partial \theta)] a^2 \sin \theta d\theta d\lambda \\ & + \int_0^\pi \int_0^{2\pi} [\zeta_c'^2 / (-\partial \bar{\zeta} / a \sin \theta \partial \theta)] a^2 \sin \theta d\theta d\lambda. \end{aligned} \quad (21)$$

Figure 11 shows the mean of F , F_d and F_c in January and July of 1982. As for the partition of the kinetic energy, the contribution of continuous-spectrum part takes the largest part. It should be pointed out that in the July case, there are points where $\partial \bar{\zeta} / \partial \theta = 0$. Since ζ_d' and ζ_c' should also be equal to zero at these points as can be inferred from (1), the defined weighted enstrophy F_d and F_c still exist.

4. Summary

In this paper, based on the analysis of spectra and spectral functions of the quasi-geostrophic model in an earlier paper (ZZ1), we have shown that observed atmospheric disturbances are largely composed of continuous-spectrum disturbances rather than discrete-spectrum disturbances. The partition of energy and weighted enstrophy between the continuous-spectrum and discrete-spectrum disturbances also shows the dominance of the continuous-spectrum part for zonal wave number $k > 3$. The discrete-spectrum disturbances make an appreciable contribution mainly in the ultra-long waves and in the tropics. It is also illustrated that the behavior of the continuous-spectrum disturbances resembles wave packets in shear basic flow. This is consistent with the fact that wave packets can be described by the continuous-spectrum disturbances.

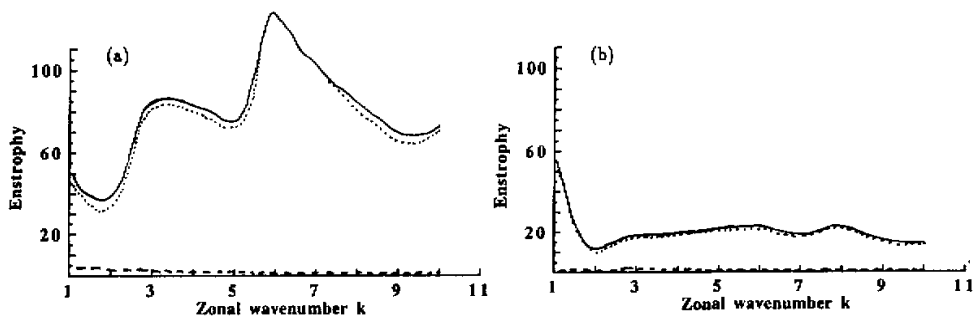


Fig. 11. Mean weighted enstrophy of the total disturbances (solid), continuous-spectrum disturbances (dotted), and the discrete-spectrum disturbances (dashed), as functions of zonal wavenumber k (ordinate) (unit is $10^{12} \text{ m}^2/\text{s}$). (a) January 1982, (b) July 1982.

These results are in agreement with previous diagnostic studies of the atmospheric general circulation about the evolution of atmospheric disturbances. For example, although freely traveling waves in the atmosphere have been reported in previous studies (eg., Madden, 1979; Kasahara, 1976), their magnitudes are very small in comparison with the atmospheric variance (Wallace and Blackman, 1983). The major component of atmospheric disturbances is dispersive in nature, interacting with the basic flow, instead of propagating freely within the basic flow. And because of this, it is plausible that continuous-spectrum disturbances also play a major role in the maintenance of the zonal basic flow. Indeed, our calculation confirms this speculation (Zeng and Zhang, 1999).

The model used in this study is the barotropic quasi-geostrophic model on the sphere. It is similar to that used in Borges and Hartmann (1992). It is applied to the 300 hPa flow in this study. Lack of baroclinic processes certainly affects the applicability of the current results. Thus, this work to project the atmospheric disturbances onto spectral functions of this model is a first step for the understanding of the barotropic effect of the shear basic flow on disturbances. It is desirable to use three-dimensional baroclinic models in the future for the derivation of spectral functions and for the diagnosis of disturbances. It is expected that spectra in a three-dimensional model are much more complicated since there exist at least two kinds of continuous spectrum. One is the barotropic one analyzed in this paper, and the other is the baroclinic one analyzed in Burger (1966) for an idealized model.

Appendix: Energy decomposition using the adjoint operator

Model (1) can be also written as:

$$(M + L)X = 0, \quad (22)$$

where

$$X = (v'_\theta, v'_\lambda, \frac{f_0}{a} \psi')^T, \quad (23)$$

and

$$L = \begin{bmatrix} \bar{\lambda} \frac{\partial}{\partial \lambda} & -2(\omega + \bar{\lambda}) \cos \theta & \frac{\partial}{\partial \theta} \\ 2(\omega + \bar{\lambda}) \cos \theta + \frac{\partial \bar{\lambda}}{\partial \theta} \sin \theta & \bar{\lambda} \frac{\partial}{\partial \lambda} & \frac{\partial}{\sin \theta \partial \lambda} \\ \frac{\partial}{\partial \theta} \sin \theta & \frac{\partial}{\partial \lambda} & 0 \end{bmatrix} \quad (24)$$

$$M = \begin{bmatrix} \frac{\partial}{\partial t} & 0 & 0 \\ 0 & \frac{\partial}{\partial t} & 0 \\ 0 & 0 & 0 \end{bmatrix}, \quad (25)$$

where $f_0 = 2\omega \sin \theta_0$, and ψ' is the stream function. Use $X = X^k e^{i(k\lambda + \sigma t)}$, an eigenvalue problem is formulated as:

$$(L_k + i\sigma M_k)X^k = 0, \quad (26)$$

where M_k is just the same M but $\partial / \partial t$ replaced by 1, and

$$\mathbf{L}_k = \begin{bmatrix} ik\bar{\lambda} & -2(\omega + \bar{\lambda})\cos\theta & \frac{\partial}{\partial\theta} \\ 2(\omega + \bar{\lambda})\cos\theta + \frac{\partial\bar{\lambda}}{\partial\theta}\sin\theta & ik\bar{\lambda} & ik\frac{1}{\sin\theta} \\ \frac{\partial}{\partial\theta}\sin\theta & ik & 0 \end{bmatrix}, \quad (27)$$

$$\mathbf{M}_k = \begin{bmatrix} 1 & 0 & 0 \\ 0 & 1 & 0 \\ 0 & 0 & 0 \end{bmatrix}. \quad (28)$$

Define an inner product of two vectors as:

$$(\mathbf{X}, \mathbf{Y}) = \int_0^\pi \mathbf{X} \mathbf{Y}^* \sin\theta d\theta, \quad (29)$$

where star represents complex conjugate, then the following operator is the adjoint operator of \mathbf{L}_k

$$\bar{\mathbf{L}}_k = \begin{bmatrix} -ik\bar{\lambda} & 2(\omega + \bar{\lambda})\cos\theta + \frac{\bar{\lambda}}{\partial\theta}\sin\theta & -\frac{\partial}{\partial\theta}\sin\theta \\ -2(\omega + \bar{\lambda})\cos\theta & -ik\bar{\lambda} & -ik \\ -\frac{\partial}{\sin\theta\partial\theta}\sin\theta & \frac{-ik}{\sin\theta} & 0 \end{bmatrix}, \quad (30)$$

such that

$$(\mathbf{L}_k \mathbf{X}^k, \mathbf{Y}^k) = (\mathbf{X}_k, \bar{\mathbf{L}}_k \mathbf{Y}^k), \quad (31)$$

where

$$\mathbf{Y}^k = (v_{\theta}^{\prime\prime k}, v_{\lambda}^{\prime\prime k}, \frac{f_0}{a} \psi^{\prime\prime k})^T. \quad (32)$$

If we write the eigenvalue and eigenvector of the adjoint operator $\bar{\mathbf{L}}_k$ as μ and \mathbf{Y}^k , then

$$(\bar{\mathbf{L}}_k - i\mu \mathbf{M}_k) \mathbf{Y}^k = 0; \quad (33)$$

and from (26), (33) and (31) we obtain

$$i(\sigma - \mu^*)(\mathbf{M}_k \mathbf{X}^k, \mathbf{M}_k \mathbf{Y}^k) = 0, \quad (34)$$

and the orthogonality of the pairs of \mathbf{X}^k and \mathbf{Y}^{k*} , i.e. $(\mathbf{M}_k \mathbf{X}^k, \mathbf{M}_k \mathbf{Y}^k) = 0$ when $\sigma \neq \mu^*$. Besides, one can take also the normalized condition when $\sigma = \mu^*$, i.e.,

$$(\mathbf{M}_k \mathbf{X}^k, \mathbf{M}_k \mathbf{Y}^k) = \int_0^\pi (v_{\theta}^{\prime k} v_{\theta}^{\prime\prime k*} + v_{\lambda}^{\prime k} v_{\lambda}^{\prime\prime k*}) \sin\theta d\theta = 1. \quad (35)$$

Since the spectrum of eigenvalues of the adjoint operator \bar{L} is the same as that of the operator L , including both the discrete spectra and the continuous spectrum, an arbitrary vector H^k ,

$$H^k = (h_1^k, h_2^k, h_3^k) \quad (36)$$

can be expanded along with either the spectral functions of L or those of \bar{L} :

$$H^k = \sum_i A_i^k X_i^k = \sum_i \bar{A}_i^k Y_i^k. \quad (37)$$

As a consequence, following (38),

$$\begin{aligned} 2E^k &= \int_0^\pi (\nu_\theta^k \nu_\theta^{k*} + \nu_\lambda^k \nu_\lambda^{k*}) \sin\theta d\theta = \sum_i \sum_{i'} A_i^k (M_k X_i^k) \bar{A}_{i'}^{k*} (M_k Y_{i'}^k) \\ &= \sum_i A_i^k \bar{A}_i^{k*} (M_k X_i^k, M_k Y_i^k) = \sum_i A_i^k \bar{A}_i^{k*} = 2E_d^k + 2E_c^k. \end{aligned} \quad (38)$$

where energy of the discrete- and that of continuous- spectrum disturbances are separated.

REFERENCES

- Ahlquist, J. E., 1982: Normal mode Rossby waves: theory and observations. *J. Atmos. Sci.*, **39**, 193–202.
- Borges, and D. L. Hartmann, 1992: Barotropic instability and optimal perturbation of observed nonzonal flows. *J. Atmos. Sci.*, **49**, 335–353.
- Burger, A. P., 1966: Instability associated with continuous spectrum in a baroclinic flow. *J. Atmos. Sci.*, **23**, 272–277.
- Charney, J. G., 1947: The dynamics of long waves in a baroclinic westerly current. *J. Meteor.*, **4**, 135–162.
- Eady, E. T., 1949: Long waves and cyclone waves. *Tellus*, **1**, 33–52.
- Farrell, B. F., 1982: The initial growth of disturbances in a baroclinic flow. *J. Atmos. Sci.*, **39**, 1663–1686.
- Farrell, B. F., 1984: Modal and non-modal baroclinic waves. *J. Atmos. Sci.*, **41**, 668–673.
- Farrell, B. F., 1985: Transient growth and damped baroclinic waves. *J. Atmos. Sci.*, **42**, 2718–2727.
- Farrell, B. F., 1988: Optimal excitation of neutral Rossby waves. *J. Atmos. Sci.*, **45**, 163–172.
- Farrell, B. F., and P. J. Ioannou, 1993: Stochastic forcing of perturbation variance in unbounded shear and deformation flows. *J. Atmos. Sci.*, **50**, 200–211.
- Held, I. M., 1985: Pseudomomentum and the orthogonality of modes in shear flows. *J. Atmos. Sci.*, **42**, 2280–2288.
- Kasahara, A., 1976: Normal modes of ultralong waves in the atmosphere. *Mon. Wea. Rev.*, **104**, 669–690.
- Lu, P. S., Lu, L., and Zeng, Q. C., 1986: Spectra of the barotropic quasi-geostrophic model and the evolutionary process of disturbances. *Scientia Sinica*, **11**, 1225–1233.
- Lu, P. S., and Zeng, Q. C., 1981: On the evolution process of disturbances in a barotropic atmosphere. *Scientia Atmospherica Sinica*, **5**(1).
- Madden, R. A., 1979: Observations of large scale traveling Rossby waves. *Rev. Geophys. and Space Phys.*, **17**, 1935–1949.
- Wallace, J. M., and M. L. Blackman, 1983: Observations of low-frequency atmospheric variability, in: *Large Scale Dynamical Processes in the Atmosphere*, Edited by: Hoskins, B. J. and Pearce, R. P., Academic Press, p55–94.
- Yoshida, K., 1980: *Functional Analysis*, 6th edition, New York: Springer-Verlag, 500pp.
- Zeng, Q. C., 1979: *The mathematical-physical basis of numerical weather prediction*. Vol. 1, Science Press, Beijing, 543pp.
- Zeng, Q. C., 1982: On the evolution and interaction of disturbances and zonal flow in rotating barotropic atmosphere. *J. Meteor. Soc. of Japan*, **60**(1): 24–31.
- Zeng, Q. C., 1983a: The evolution of Rossby wave packet in a three-dimensional baroclinic atmosphere. *J. Atmos.*

- Sci.*, **40**, 73–84.
- Zeng, Q. C., 1983b: The development characteristics of quasi-geostrophic baroclinic disturbances. *Tellus*, **35A**, 337–349.
- Zeng, Q. C., Lu, P. S., Li, R. F., and Yuan C. G., 1986: Evolution of large scale disturbances and their interactions with mean flow in a rotating atmosphere, Parts 1 and 2. *Adv. Atmos. Sci.*, **3**, 38–58, 171–188.
- Zeng, Q. C., and Zhang M. H., 1999: Wave-mean flow interaction: the role of continuous-spectrum disturbances. (to appear in AAS).
- Zhang, M. H., and Zeng Q.C., 1997: Discrete spectra and continuous spectrum of the barotropic quasi-geostrophic model, Part I. *J. Atmos. Sci.*, **54**, 1910–1922.